

Observation of Antiparallel Magnetic Order in Weakly Coupled Co/Cu Multilayers

J. A. Borchers, J. A. Dura, J. Unguris, D. Tulchinsky, M. H. Kelley, and C. F. Majkrzak
National Institute of Standards and Technology, Gaithersburg, Maryland 20899

S. Y. Hsu, R. Loloee, W. P. Pratt, Jr., and J. Bass

Department of Physics and Astronomy, Michigan State University, East Lansing, Michigan 48824
 (Received 16 December 1998)

Polarized neutron reflectivity and scanning electron microscopy with polarization analysis are combined to determine the magnetic structure of Co(6 nm)/Cu(6 nm) multilayers. These data resolve a controversy regarding the low-field state of giant-magnetoresistive (GMR) multilayers with weak coupling. As-prepared samples show a strong antiparallel correlation of in-plane ferromagnetic Co domains across the Cu. At the coercive field, the Co domains are uncorrelated. This irreversible transition explains the decrease in magnetoresistance from the as-prepared to the coercive state. For both states, the Co moments reside in domains with in-plane sizes of $\approx 0.5\text{--}1.5\ \mu\text{m}$. [S0031-9007(99)08797-9]

PACS numbers: 75.70.Cn, 61.12.Ha, 75.60.Ch, 75.70.Pa

The combination of polarized neutron reflectivity (PNR) and scanning electron microscopy with polarization analysis (SEMPA) represents a powerful tool for studying magnetic order in materials with buried magnetic layers, such as multilayers composed of alternating layers of ferromagnetic and nonmagnetic metals. PNR probes the order of the entire sample, while SEMPA produces a direct image of the magnetic domain structure within one magnetic layer at a time. In this Letter, we report the successful use of PNR and SEMPA to resolve a controversy in giant magnetoresistance (GMR) in Co/Cu multilayers.

The resistance (R) of a GMR multilayer greatly decreases when an external field (H) reorients the in-plane magnetizations of the ferromagnetic layers parallel (P) to each other [1]. The magnetoresistance, $\text{MR}(H) = [R(H) - R(P)]/R(P)$, is largest for systems in which $R(H)$ at a low field is associated with antiparallel alignment of adjacent ferromagnetic layers. Theoretical analysis has focused upon this maximum MR [2].

Increasing the thickness of the nonmagnetic layer, t_n , can lead to an oscillation between antiparallel and parallel states with respectively large and small MR [3]. The strength of the exchange coupling between the ferromagnetic layers decreases with increasing t_n . For weak interlayer coupling ($t_n > 4\text{--}5\ \text{nm}$), the magnetoresistance $\text{MR}(0)$ for the as-prepared multilayer is often larger than the maximum value at the coercive field $\text{MR}(H_C)$ after saturation [4]. $\text{MR}(0)$ usually cannot be restored by field cycling or by demagnetization [5,6]. Because $\text{MR}(H_C)$ reproduces upon cycling, most investigators have assumed that it approximates the antiparallel state [7].

We have performed PNR and SEMPA measurements on Co/Cu multilayers with Cu layers thick enough ($t_{\text{Cu}} = 6\ \text{nm}$) that the exchange coupling between the Co layers is weak. We find that $\text{MR}(0)$ originates from strong antiparallel correlations among the Co domain magnetizations across the Cu layers. In contrast, $\text{MR}(H_C)$ and MR af-

ter demagnetization are both associated with uncorrelated domains in adjoining Co layers. In the as-prepared state, the antiparallel correlation occurs within small columnar Co domains with an average in-plane size of $0.5\text{--}1.5\ \mu\text{m}$. This domain size is essentially unchanged at H_C and after the sample is demagnetized.

We focus on a multilayer of nominal composition $[\text{Co}(6\ \text{nm})|\text{Cu}(6\ \text{nm})]_{20}$, but supporting PNR results were obtained on additional samples. The sample was sputtered onto a $1 \times 1\ \text{cm}^2$ Si substrate as described elsewhere [8]. Specular x-ray reflectivity confirms that the Co and Cu layers are well modulated. The field dependence of the magnetization and magnetoresistance were measured at room temperature for a "twin" sample grown at the same time. SQUID (superconducting quantum interference device) magnetometer measurements indicate that the Co moments preferentially lie in the layer plane. The magnetization saturates in an in-plane field of approximately 200 Oe. As shown in Fig. 1, the room temperature current-in-plane $\text{MR}(0)$ is 6.6%, whereas $\text{MR}(H_C)$ is only 4.0%. This ratio of $\text{MR}(0)/\text{MR}(H_C)$ typifies those of sputtered Co/Cu multilayers with similar Co and Cu thicknesses both at room temperature and 4.2 K [4].

We performed PNR studies at room temperature on the NG-1 reflectometer at the NIST Center for Neutron Research. These data are sensitive to the size, in-plane orientation, and relative interlayer alignment of magnetic domains in buried layers [9–12]. For specular and diffuse (i.e., off-specular) experiments, we measured all four cross sections, $(--)$, $(++)$, $(+-)$, and $(-+)$. (The $+$ and $-$ signs indicate polarizations of the incident and scattered neutrons parallel or antiparallel to the external field.) The $(--)$ and $(++)$ non-spin-flip (NSF) data depend on the chemical structure, as well as the projection of the in-plane magnetization parallel to the applied field. The $(+-)$ and $(-+)$ spin-flip (SF) cross sections arise solely from the projection of the in-plane magnetization perpendicular to

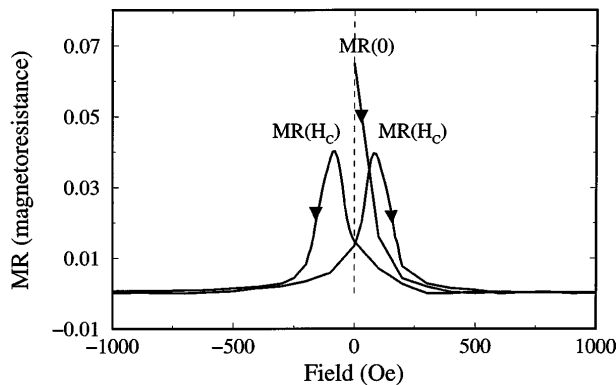


FIG. 1. Current-in-plane magnetoresistance measurements for the $[\text{Co}(6 \text{ nm})|\text{Cu}(6 \text{ nm})]_{20}$ multilayer at room temperature. The magnetoresistance of the as-prepared and coercive states are marked.

this field [9]. We note that the efficiencies of the NG-1 neutron polarizers were $>95\%$ in external fields as small as 1.5 Oe.

Figure 2 shows total reflectivity scans along the Q_z direction relative to the diffuse scattering for the $[\text{Co}(6 \text{ nm})|\text{Cu}(6 \text{ nm})]_{20}$ sample in the as-prepared state (a) and at the coercive field, H_C (b). In both cases, the NSF total reflectivity data have a first-order structural superlattice peak at $Q_z = 0.057 \text{ \AA}^{-1} \approx 2\pi/d$, where $d = 11.4 \text{ nm}$ is the bilayer repeat distance. Figure 2(a) also shows a pronounced magnetic peak in all four cross sections at the half-order position ($Q_z = 0.031 \text{ \AA}^{-1} \approx 2\pi/2d$). The magnetic repeat distance in the as-prepared state is *twice* the bilayer thickness d ; i.e., a large fraction of the Co layer moments are oriented antiparallel along the growth axis. The narrow Q_z width of the half-order reflection reveals that this antiparallel order is coherent through the entire multilayer thickness. The half-order peak has a substantial diffuse component (open symbols), which originates from discrete domains spread over the layer plane [12,13]. The in-plane direction of these domains within the sample plane is likely random since the diffuse magnetic intensity in the half-order reflection is evenly distributed in all four cross sections. The as-prepared state thus has ferromagnetic, in-plane domains that are oriented antiparallel across the intervening Cu layers, as depicted in the inset of Fig. 2(a).

In Fig. 2(a), the SF scattering at the first-order position is large relative to that in Fig. 2(b), which originates entirely from the finite efficiencies of the instrumental polarizers. A fit to the data indicates that the excess scattering results from a small fraction ($<3\%$) of the total Co moments in the sample that are aligned parallel across the intervening Cu. Since data for comparable Co/Cu and Co/Ag samples [14] showed no excess of SF scattering at the first-order position in the as-prepared state, the dominant antiparallel Co configuration is undoubtedly responsible for the maximum $\text{MR}(0)$ in Fig. 1.

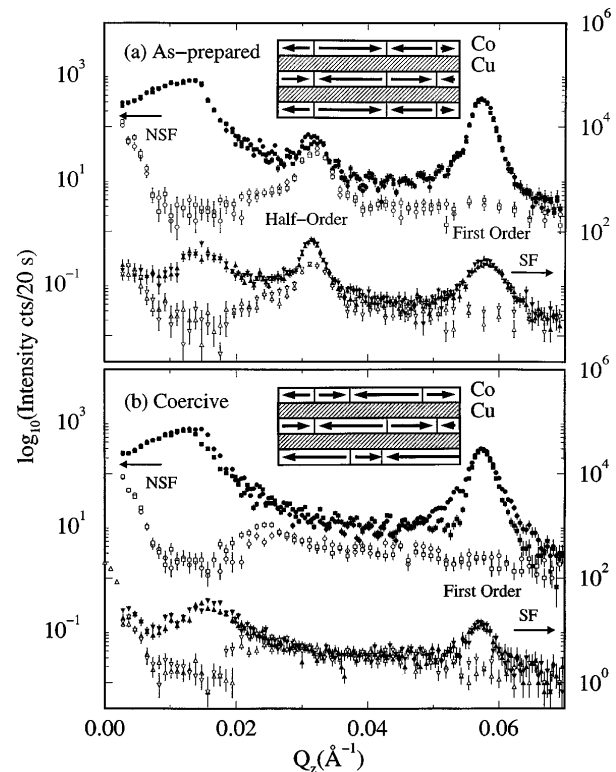


FIG. 2. Total PNR (shaded symbols) relative to the diffuse scattering (open symbols) as a function of $Q_z = 4\pi/\lambda \sin \theta$ for $[\text{Co}(6 \text{ nm})|\text{Cu}(6 \text{ nm})]_{20}$ in the (a) as-prepared and (b) coercive state at $H_C = 54 \text{ Oe}$. The diffuse scattering was measured by offsetting the angle Ω by 0.2° and then scanning Q_z . The circles and squares correspond to $(-)$ and $(+)$ NSF data, respectively. The up and down triangles mark the $(+)$ and $(-)$ SF data. No corrections have been made for the polarization efficiencies or sample footprint. The insets show the idealized magnetic structures suggested by the scattering in each state.

In accord with the magnetoresistance data in Fig. 1, application of a field irreversibly destroys the antiparallel order. The half-order reflection in Fig. 2(a) disappeared when the sample was saturated in a -375 Oe field and, as shown in Fig. 2(b), it did not reappear when the sample was taken to the coercive field ($H_C = 54 \text{ Oe}$). Instead, diffuse magnetic scattering (i.e., in the SF cross sections) is distributed over a wide range of Q_z values between 0.02 and 0.05 \AA^{-1} . In the coercive state, the Co moments in all samples seem to order in domains with small in-plane dimensions that are not magnetically correlated with adjoining Co layers [inset of Fig. 2(b)]. The consequence is that $\text{MR}(H_C)$ is less than $\text{MR}(0)$. Moreover, demagnetizing the sample yielded zero-field PNR data resembling the coercive-state data in Fig. 2(b). The initial antiparallel configuration was not restored by either field cycling or demagnetization.

The strong antiparallel interlayer ordering in the as-prepared state was confirmed by SEMPA with ion milling, which allows direct imaging of the magnetic domain

structure in successive Co layers of the as-prepared sample. By measuring the secondary electron spin polarization in a scanning electron microscope, SEMPA can sense the surface magnetization and, simultaneously, the topography of a magnetic sample [15]. *In situ* ion sputtering using 2 keV Ar⁺ ions was used to clean and depth profile the sample. Figures 3(a) and 3(b) are SEMPA images of the magnetization and topography, respectively, of the outermost Co layer after removing the protective Cu overlayer. The SEMPA topographic image reveals structural grain sizes that are about 0.1 μm . In comparison, Fig. 3(a) shows irregular magnetic domains with feature sizes generally on the order of a micron, along with Néel-like domain walls about 0.2 μm wide with random chirality. We note that the domain magnetizations in the imaged region are predominantly aligned along one direction, but this uniaxial anisotropy is not evident in the PNR measurements which probe the entire sample area. It is thus possible that the anisotropy direction varies with lateral or vertical position.

Figure 3(c) shows a SEMPA image from the second Co layer after removing the top Co and Cu layers. The domain structure of this layer is strongly anticorrelated with that of the outermost layer in Fig. 3(a). The anticorrelation even extends to such small features as the domain walls, which preserve chirality in the adjoining layer. [An example is highlighted by the arrows in Figs. 3(a) and 3(c).] The degree of correlation in the area shown is quantified in a histogram shown in Fig. 3(d) of the difference in

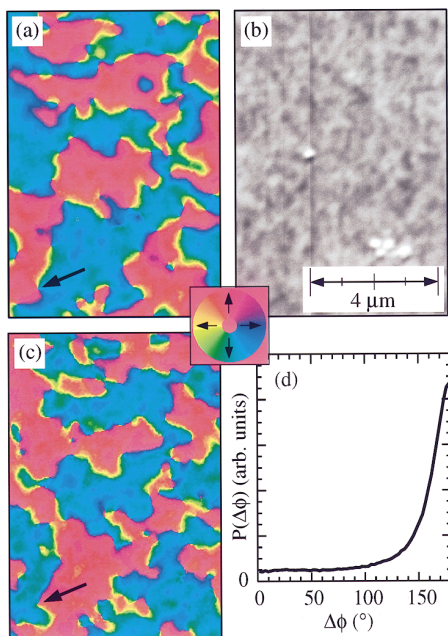


FIG. 3(color). SEMPA images of the topmost Co layer magnetization (a) and topography (b) and second Co layer magnetization (c) in the $[\text{Co}(6\text{ nm})|\text{Cu}(6\text{ nm})]_{20}$ sample. The magnetization direction is mapped to color as indicated by the color wheel in the center. A histogram of the difference in the magnetization direction between the two layers, $\Delta\phi$, is shown in (d).

magnetization direction, $\Delta\phi$, between the two Co layers. The histogram shows that about 60% of the domains are aligned antiparallel (within $\approx 20^\circ$), while the rest are uncorrelated.

Because SEMPA cannot be used in a field, we could not image the sample at H_C . Instead, we examined it after demagnetization, which, as shown by PNR, produces a state analogous to the uncorrelated coercive state of Fig. 2(b). A histogram of the SEMPA data revealed that the magnetizations of the top two Co layers are uncorrelated, as expected.

Figures 3(a) and 3(c) indicate that the average domain size in a local region of the sample is on the order of a micron. This value matches that obtained from PNR, which probes the entire sample. Figure 4 shows SF data for transverse Q_x scans centered at the half-order position ($Q_z = 0.0314\text{ \AA}^{-1}$) for $[\text{Co}(6\text{ nm})|\text{Cu}(6\text{ nm})]_{20}$ in the as-prepared, coercive, and saturated states. (The NSF data are similar.) The as-prepared and coercive data in Fig. 4 are composed of a sharp specular reflection at $Q_x = 0\text{ \AA}^{-1}$ on top of a broad, diffuse peak. Dips are centered at the sample angles $\Omega = 0$ and $\Omega = 2\theta$ where either the incident or scattered beam is parallel to the sample face and is thus reflected (or refracted) out of the sample or detector, respectively. Since the SF cross section is purely magnetic in origin and the instrumental polarization efficiency is $>95\%$, the diffuse scattering principally originates from magnetic, rather than structural, features within the sample plane. This conclusion is supported by the decrease of the SF scattering to background levels when the Co moments are aligned in a saturation field of 400 Oe (Fig. 4). We believe that these data are among the best examples of magnetic diffuse scattering from buried layers obtained

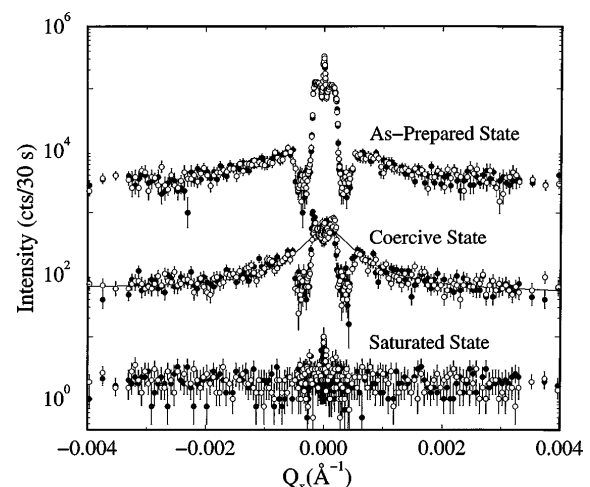


FIG. 4. Transverse Q_x scans at the half-order position ($Q_z = 0.0314\text{ \AA}^{-1}$) for $[\text{Co}(6\text{ nm})|\text{Cu}(6\text{ nm})]_{20}$ in the as-prepared, coercive ($H_C = 54\text{ Oe}$) and saturated ($H = 400\text{ Oe}$) states. The data for each state have been offset by $10^{1.5}$ for clarity. Only the (+-) and (-+) SF cross sections are shown (shaded and open circles, respectively). The coercive-state data have been fit to a Lorentz function (solid line).

by either neutron reflectivity [11,13,16] or x-ray resonant scattering [17] techniques.

The full width of the SF diffuse peak is inversely related to an in-plane magnetic correlation length, which generally corresponds to an average domain size [12]. A fit of the peak in the coercive-state data (Fig. 4) to a Lorentz function gives an estimated length of 0.5–1.5 μm in good agreement with the SEMPA data in Fig. 3. Since the overall width of the diffuse data for the coercive state and the as-prepared state are similar, the magnetic correlation lengths for the $[\text{Co}(6\text{ nm})|\text{Cu}(6\text{ nm})]_{20}$ sample are nearly the same in these two states. However, subtle differences in the two line shapes suggest that the details of the in-plane magnetic structure are sensitive to field history. For example, the central specular peak at $Q_x = 0\text{ \AA}^{-1}$ is quite pronounced for the as-prepared state relative to the coercive state. The coexistence of the diffuse and specular peaks implies that the small, micron-order domains are mixed with larger domains (i.e., in-plane dimensions $\geq 100\text{ \mu m}$) that are aligned antiparallel across the Cu layers in the as-prepared state. The latter disappear upon field cycling and cannot be restored, even after demagnetizing the sample.

As to the origin of the magnetic ordering in the as-prepared state, we speculate that dipolar interactions arising from the fields at the edges of the micron-sized domains in one Co layer may be strong enough [11] to induce local antiparallel alignment of the growing domains in the next Co layer. The resulting structure consists of columns of domains within which the Co layer magnetizations, including the domain wall directions [Figs. 3(a) and 3(c)], are aligned antiparallel. Once a layer is complete and covered by additional layers, the dipolar forces become secondary relative to intralayer exchange coupling and domain wall pinning due to structural defects. After field cycling, these interactions inhibit the development of antiparallel alignment as the Co magnetization relaxes. Alternately, magnetic anisotropy might trap the multilayer in local energy minima [18].

In summary, we have characterized the magnetic structure of a $\text{Co}(6\text{ nm})|\text{Cu}(6\text{ nm})$ multilayer with weak interlayer coupling using the complementary techniques of PNR, which simultaneously probes all Co layers, and SEMPA, which examines one Co layer at a time. Together, these measurements reveal that the average in-plane domain sizes in the as-prepared, coercive, and demagnetized states are all approximately 1 μm . These domains have strong antiparallel ordering across the Cu layers in the as-prepared state, whereas the ordering is more nearly random in the coercive and demagnetized states. Antiparallel ordering of the Co is thus responsible for the large magnetoresistance $\text{MR}(0)$ in the as-prepared state, relative to that of the coercive state $\text{MR}(H_C)$.

We appreciate discussions with J.F. Ankner, M.D. Stiles, and R.J. Celotta. Research was supported by NSF DMR-9423795, MRSEC Program DMR-9400417, MSU-CFMR, and Ford Research Laboratory.

-
- [1] M.N. Baibich, J.M. Broto, A. Fert, F. Nguyen Van Dau, F. Petroff, P. Etienne, G. Creuzet, A. Friederich, and J. Chazelas, *Phys. Rev. Lett.* **61**, 2472 (1988).
 - [2] P.M. Levy, in *Solid State Physics*, edited by H. Ehrenreich and D. Turnbull (Academic, New York, 1994), Vol. 47, p. 367.
 - [3] S.S.P. Parkin, N. More, and K.P. Roche, *Phys. Rev. Lett.* **64**, 2304 (1990); S.S.P. Parkin, R. Bhadra, and K.P. Roche, *Phys. Rev. Lett.* **66**, 2152 (1991).
 - [4] W.P. Pratt, Jr., S.-F. Lee, J.M. Slaughter, R. Loloee, P.A. Schroeder, and J. Bass, *Phys. Rev. Lett.* **66**, 3060 (1991).
 - [5] P.A. Schroeder, S.-F. Lee, P. Holody, R. Loloee, Q. Yang, W.P. Pratt, Jr., and J. Bass, *J. Appl. Phys.* **76**, 6610 (1994).
 - [6] Ch. Rehm, F. Klose, D. Nagengast, B. Pietzak, H. Malletta, and A. Weidinger, *Physica (Amsterdam)* **221B**, 377 (1996).
 - [7] See, e.g., S.S.P. Parkin, A. Modak, and D.J. Smith, *Phys. Rev. B* **47**, 9136 (1993); B. Doudin, A. Blondel, and J.-Ph. Ansermet, *J. Appl. Phys.* **79**, 6090 (1996); L. Piraux, S. Dubois, C. Marchal, J.M. Beuken, L. Filippozzi, J.F. Despres, K. Ounadjela, and A. Fert, *J. Magn. Mater.* **156**, 317 (1996).
 - [8] J.M. Slaughter, W.P. Pratt, Jr., and P.A. Schroeder, *Rev. Sci. Instrum.* **60**, 127 (1989).
 - [9] C.F. Majkrzak, *Physica (Amsterdam)* **221B**, 342 (1996).
 - [10] S.K. Sinha, E.B. Sirota, S. Garoff, and H.B. Stanley, *Phys. Rev. B* **38**, 2297 (1988); V. Holý and T. Baumbach, *Phys. Rev. B* **49**, 10668 (1994).
 - [11] J.A. Borchers, P.M. Gehring, R.W. Erwin, J.F. Ankner, C.F. Majkrzak, T.L. Hylton, K.R. Coffey, M.A. Parker, and J.K. Howard, *Phys. Rev. B* **54**, 9870 (1996).
 - [12] S.K. Sinha in *Neutron Scattering in Materials Science II*, edited by D.A. Neumann, T.P. Russell, and B.J. Wuenesch, Materials Research Society Symposium Proceedings Vol. 376 (Materials Research Society, Pittsburgh, 1995), p. 175.
 - [13] G.P. Felcher, *Physica (Amsterdam)* **192B**, 137 (1993).
 - [14] J.A. Borchers, J.A. Dura, C.F. Majkrzak, S.Y. Hsu, R. Lolee, W.P. Pratt, Jr., and J. Bass (unpublished).
 - [15] M.R. Scheinfein, J. Unguris, M.H. Kelley, D.T. Pierce, and R.J. Celotta, *Rev. Sci. Instrum.* **61**, 2501 (1990).
 - [16] M. Takeda, Y. Endoh, H. Yasuda, K. Yamada, A. Kamijo, and J. Mizuki, *J. Phys. Soc. Jpn.* **62**, 3015 (1993).
 - [17] J.F. MacKay, C. Teichert, D.E. Savage, and M.G. Lagally, *Phys. Rev. Lett.* **77**, 3925 (1996).
 - [18] H. Holloway and D.J. Kubinski, *J. Appl. Phys.* **83**, 2705 (1998).